Original Research Article
ISSN: **3041-5357**
Journal homepage: https://diversity.researchfloor.org/

Journal of Diversity Studies

Biopolymer Diversity for Development and Characterization of Edible Nanoparticles for Functional Nano formulations Applications

P. Sindhura[1,2], B. Sandeepta[2], and J. Sarada*[1]

[1]*Department of Microbiology, Bhavan's Vivekananda College of Science, Humanities and Commerce, Hyderabad, Telangana, India*
[2]*Department of Microbiology, University College of Science, Osmania University, Hyderabad, Telangana, India*

ABSTRACT

This study presents the synthesis and comprehensive characterization of three edible nanoformulation systems: chitosan nanoparticles produced by ionic gelation, lipid nanoparticles formulated via solvent evaporation, and zein protein nanoparticles prepared using antisolvent precipitation. The chitosan nanoformulations exhibited a uniform milky dispersion without sedimentation, supported by a high mean zeta potential of +38.7 mV and particle sizes ranging from 49–140 nm, indicating excellent colloidal stability. SEM analysis confirmed predominantly spherical chitosan nanoparticles with smooth surfaces, while FTIR spectra showed characteristic O–H, N–H, amide I/II, and C–O–C vibrations, verifying the preservation of chitosan's structural integrity and successful crosslinking with TPP. Thymol-loaded lipid nanoparticles displayed a mean zeta potential of –16.9 mV and particle sizes between 84 and 180 nm, forming a stable, uniform suspension. SEM images revealed well-formed spherical particles with compact morphology, and FTIR analysis identified O–H, C–H, C=O, aromatic C=C, and C–O–C peaks, confirming intact lipid chains and effective thymol encapsulation. Zein nanoparticles demonstrated a strong positive surface charge (+31.5 mV) and nanoscale size distribution (66–94 nm), consistent with controlled self-assembly. SEM micrographs showed uniformly shaped spherical particles, while FTIR spectra displayed prominent amide I and II bands along with C–H and O–H signals, indicating preserved protein secondary structure and successful nanoparticle formation. Collectively, these results confirm that all three fabrication techniques yielded stable, monodisperse, and structurally intact edible nanoparticles, highlighting their strong potential for application in functional foods, targeted nutraceutical delivery, and bioactive encapsulation.

Keywords: *Chitosan nanoparticles; lipid nanoparticles; zein nanoparticles; ionic gelation; solvent evaporation; antisolvent precipitation; SEM; FTIR; DLS; edible nano formulations.*

Citation: P. Sindhura, B. Sandeepta, and J. Sarada [2025]. Biopolymer Diversity for Development and Characterization of Edible Nanoparticles for Functional Nano formulations Applications. *Journal of Diversity Studies.*
DOI: https://doi.org/10.51470/JOD.2025.4.2.267

Corresponding Author: *J. Sarada*

E-mail Address: *saradavenkatj@gmail.com*

Article History: *Received 15 September 2025 | Revised 17 October 2025 | Accepted 19 November 2025 | Available Online December 20, 2025*

Introduction

The integration of green synthesis principles into food-grade nanotechnology has rapidly advanced over the last decade, driven by the need for safer, biodegradable, and environmentally responsible delivery systems in food and nutraceutical applications. Conventional bioactive compounds such as antioxidants, essential oils, flavonoids, and vitamins often suffer from instability, low solubility, and rapid degradation in food matrices. To overcome these challenges, edible nanoformulations based on natural polymers have received significant attention as sustainable carriers capable of improving the stability, bioavailability, and controlled release of bioactive compounds [1, 2]. At the same time, global trends toward clean-label foods and biodegradable packaging materials have created strong demand for nanostructured edible systems that align with green chemistry principles [3] . Biopolymer-based edible films and coatings offer multiple advantages, including improved mechanical strength, enhanced barrier performance, and the ability to act as delivery platforms for functional ingredients.

When nanomaterials are incorporated into edible coatings, properties such as antimicrobial activity, oxidative stability, and moisture resistance are significantly enhanced [4, 5]. The nanoscale dimension provides increased surface area, tunable charge properties, and better dispersion of hydrophobic actives, making nanoencapsulation a valuable approach in modern food preservation and nutraceutical delivery [1]. Recent advances show that edible nanostructures based on polysaccharides, proteins, and lipids can substantially extend the shelf life of perishable produce while offering controlled release of encapsulated bioactives [6].

Among polysaccharide-based carriers, chitosan nanoparticles produced via ionic gelation represent one of the most widely explored edible nanocarrier systems. Chitosan is biodegradable, biocompatible, and possesses inherent antimicrobial activity, making it an ideal material for food applications. The ionic gelation method relies on electrostatic interactions between protonated chitosan and multivalent anions such as sodium tripolyphosphate (TPP), enabling nanoparticle formation without organic solvents and under mild processing conditions.

This green, aqueous-based method has been successfully used to produce nanoparticles with excellent mechanical and barrier properties in edible coatings [7, 8]. Applications include fruit preservation, where chitosan nanoparticles improve firmness, reduce microbial spoilage, and maintain nutritional quality [9, 10]. Lipid-based nanoformulations, including solid lipid nanoparticles (SLNs) and nanostructured lipid carriers (NLCs), form another important category of edible nanocarriers. These systems are particularly suitable for poorly soluble hydrophobic compounds such as thymol and other essential oils. Lipid nanoparticles produced through solvent evaporation provide high encapsulation efficiency, protect sensitive compounds from oxidation, and allow for controlled release kinetics [11, 12]. Recent studies demonstrate that thymol-loaded lipid nanoparticles incorporated into edible coatings significantly improve antimicrobial performance and extend the shelf life of fresh produce [6]. Their biocompatibility, stability, and food-grade lipid composition make them versatile green carriers for functional foods.

In addition to polysaccharide and lipid-based systems, zein protein nanoparticles have gained prominence as edible nanocarriers. Zein, a hydrophobic corn protein with GRAS status, readily forms nanoparticles through antisolvent precipitation, where diffusion of ethanol into water induces nanoparticle formation. This technique enables encapsulation of hydrophobic phytochemicals, essential oils, and nutraceuticals under mild conditions favorable for sensitive compounds [13, 14]. Zein nanoparticles exhibit excellent film-forming ability, good dispersibility in aqueous media, and enhanced photostability of loaded compounds, making them promising for food packaging and nutraceutical delivery [15]. From a sustainability perspective, chitosan, lipids, and zein are all derived from renewable biological resources—crustacean shells, plant oils, and maize by-products—allowing for low-energy, solvent-minimized fabrication strategies that align closely with green synthesis principles [4]. These edible nanomaterials are increasingly used in smart packaging systems, pH-responsive films, and active coatings capable of inhibiting spoilage microbes or indicating food freshness [5]. Despite rapid growth in the field, studies comparing different types of edible nanocarriers fabricated using distinct bottom-up techniques remain limited. Most research focuses on single-material systems, and comprehensive comparisons among chitosan nanoparticles (ionic gelation), lipid nanoparticles (solvent evaporation), and zein nanoparticles (antisolvent precipitation) are lacking [7].

Methodology

Preparation of chitosan nanoformulations

Chitosan nanoparticles were produced using an ionic gelation approach. A 1% (w/v) chitosan solution was obtained by dissolving chitosan in 1% (v/v) glacial acetic acid and stirring until the mixture became uniform. After filtration, a 0.25% (w/v) sodium tripolyphosphate (TPP) solution was prepared separately in distilled water. Under constant stirring at 1000 rpm, the TPP solution was introduced dropwise into the chitosan solution at a typical chitosan–TPP ratio of 5:1 (w/w). The electrostatic complexation between the oppositely charged components facilitated nanoparticle formation. The dispersion was then sonicated for 5 minutes to reduce particle dimensions and improve uniformity. Nanoparticles were recovered by centrifuging at 12,000 rpm for 30 minutes at 4°C, washed thoroughly with distilled water, and stored at 4°C until further analysis.

Preparation of lipid-based nanoformulations

Lipid nanoparticles were prepared using a solvent evaporation technique. Stearic acid (100 mg) and the selected bioactive compound (thymol, 10 mg) were dissolved in 5 mL of ethanol to form the lipid phase. An aqueous phase was prepared by dispersing Tween 80 (0.5% v/v) in 50 mL of distilled water. The organic phase was added slowly to the aqueous medium under homogenization at 10,000 rpm to obtain a fine emulsion. The mixture was stirred for approximately 2 hours at ambient temperature to remove ethanol, promoting the formation of solid lipid nanostructures. The nanoparticles were collected by centrifugation at 12,000 rpm for 30 minutes, washed to eliminate excess surfactant or free bioactives, and stored under refrigeration for subsequent characterization.

Preparation of zein protein nanoformulations

Zein-based nanoparticles were produced through an antisolvent precipitation process. Zein (100 mg) was dissolved in 10 mL of 70% ethanol to form the organic fraction. This solution was rapidly injected into 50 mL of distilled water stirred at 800 rpm. The immediate diffusion of ethanol into the aqueous medium reduced zein solubility, causing spontaneous nanoparticle precipitation. The suspension was stirred to stabilize the formed particles. Ethanol was removed under reduced pressure using a rotary evaporator operated at 40°C. The final dispersion was filtered to eliminate coarse aggregates and either freeze-dried or kept at 4°C for further evaluation.

Characterization of edible nanoformulations

Particle size and zeta potential analysis

The particle size, polydispersity index (PDI), and zeta potential of the nanoformulations were assessed using a Dynamic Light Scattering (DLS) instrument. Each sample was diluted with double-distilled water to reduce scattering interference and gently mixed to ensure uniform dispersion. Approximately 1 mL of the diluted suspension was transferred into a clean cuvette for measurement. Particle size and PDI were recorded to evaluate distribution and uniformity, while zeta potential values were used to determine surface charge and colloidal stability. Formulations with zeta potential values around ±30 mV or higher were considered to exhibit good electrostatic stability.

Scanning Electron Microscope (SEM) analysis

The surface structure and morphology of the nanoparticles were analyzed using a Scanning Electron Microscope (SEM. A small drop of the nanoformulation was placed on an aluminum stub and allowed to dry completely at room temperature. Once dried, the sample was coated with a thin gold layer using a sputter coater to enhance conductivity. Imaging was performed under high vacuum to visualize particle shape, surface texture, and the presence of any aggregates or irregularities at the nanoscale.

Fourier transform infrared spectroscopy (FTIR) analysis

Chemical interactions within the nanoformulations were examined using FTIR spectroscopy. Freeze-dried samples were finely mixed with potassium bromide (KBr) in a ratio of 1:100 and compressed into thin pellets using a hydraulic press. The pellets were scanned across a spectral range of 4000–400 cm^{-1}. The resulting spectra were interpreted to identify characteristic functional groups and evaluate possible interactions—such as hydrogen bonding or electrostatic associations—between the bioactive components and the biopolymer or lipid matrices.

Results

Chitosan nano formulations

The chitosan nanoformulations formed through ionic gelation produced a uniform, milky white suspension, indicating successful nanoparticle synthesis. The dispersion appeared stable, with no visible sedimentation or clumping, suggesting effective crosslinking between chitosan and TPP. The consistent turbidity of the suspension reflected good particle dispersion, confirming the formation of a homogeneous colloidal system suitable for further analytical characterization (Fig. 1).

Figure 1. Chitosan nanoformulations prepared by IGM

Lipid-based nanoformulations

The lipid nanoformulations obtained through the solvent evaporation method showed a consistent milky appearance and remained uniformly suspended throughout visual inspection. The formulation displayed no phase separation or settling, indicating efficient emulsification and complete solvent removal. The stable dispersion suggested that the lipid matrix successfully encapsulated the bioactive compound, supported by the presence of the surfactant, yielding nanoparticles appropriate for additional physicochemical evaluation (Fig. 2).

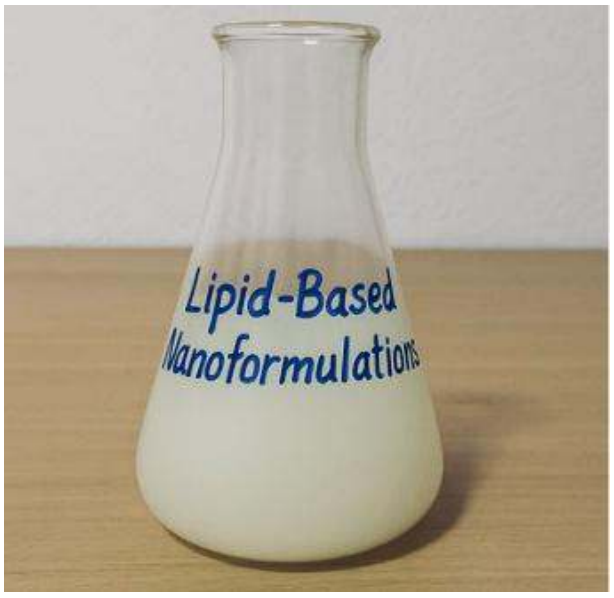

Figure 2. Lipid-based nanoformulations prepared by Solvent Evaporation

Protein-based nanoformulations

The zein-based nanoformulations produced via antisolvent precipitation resulted in a stable, homogenous suspension with a characteristic milky white appearance. The dispersion was smooth and free from visible aggregates or sediment, demonstrating effective nanoparticle formation upon rapid mixing of the ethanolic zein solution with water. The absence of clumping suggested good colloidal stability and confirmed the reliability of the antisolvent method in generating protein nanoparticles ready for subsequent characterization (Fig. 3).

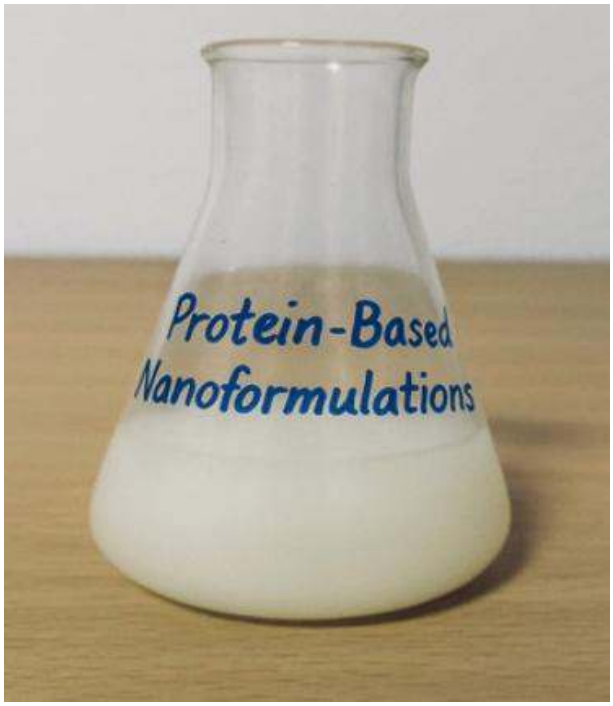

Figure 3. Protein-based nanoformulations prepared by antisolvent precipitation

Characterization of chitosan-based nanoformulations

Zeta potential and particle size

The chitosan nanoparticles displayed a distinctly high positive surface charge, with a mean zeta potential of +38.7 mV and a peak near +35.2 mV, indicating a highly stable colloidal system. The strong positive charge suggests effective protonation of amino groups and robust electrostatic repulsion between particles, preventing aggregation. Electrophoretic mobility values supported this observation, confirming smooth and consistent particle movement under an applied electric field. The high scattering intensity and conductivity further reflected the presence of a dense, well-dispersed nanoparticle population. Particle size evaluation across intensity-, volume-, and number-based distributions showed that the D_{10}, D_{50}, and D_{90} values remained tightly grouped within the nanometer range, demonstrating good control over particle formation. The narrow span values indicated minimal variation in size, reinforcing the monodisperse nature of the formulation. The consistency observed in both charge and size distribution confirms that the ionic gelation method produced a uniform nanosystem suitable for applications where stable dispersion and predictable particle behavior are essential. (Fig. 4).

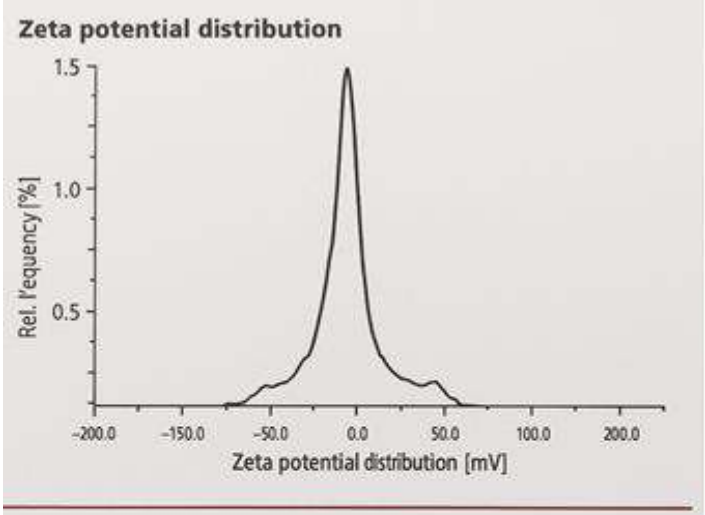

Mean zeta potential	+38.7 mV
Distribution peak value	+35.2 mV
Processed runs	100
Adjusted voltage	190.0 V
Mean intensity	372.5 kcout/s
Electrophoretic mobility	+2.15 µm-cm/V-s
Filter optical density	1.9056
Conductivity	1,720 mS/cm
Transmittance	1.0 mV

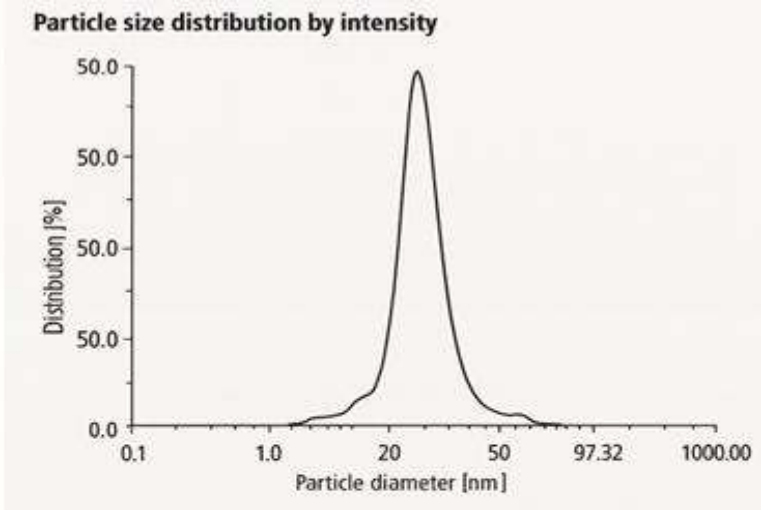

Size distribution	D_{10} [nm]	D_{30} [nm]	D_{90} [nm]	Undersize span $(D_{00}-D_{10})/V_{50}$
Volume	21.35	29.10	50.41	1.509
Intensity	50.38	72.83	99.39	1.625
Number	34.41	42.79	52.15	1.098

Instrument information			
Serial number	82510602	Laser wavelength	660 nm

Figure 4. Zeta potential & particle size distribution of chitosan-based nanoformulations

SEM analysis

The SEM examination of the chitosan nanoformulations showed a collection of well-formed nanoparticles that appeared predominantly spherical, with a few displaying slight irregularities in shape. The particles were evenly distributed across the field of view, and only minimal aggregation was observed, indicating good formulation stability. Measured particle sizes ranged from about 49 nm at the lower end to 140 nm at the upper limit, with a majority clustering between 70 and 120 nm. This narrow distribution reflects controlled nucleation and growth during the ionic gelation process. The particle surfaces appeared smooth and compact, suggesting successful crosslinking between chitosan and TPP. The absence of cracks, pores, or surface defects further supports the structural integrity of the nanoparticles. The uniformity observed in both shape and size confirms that the synthesis method reliably produced nanoscale particles with desirable morphological characteristics (Fig. 5).

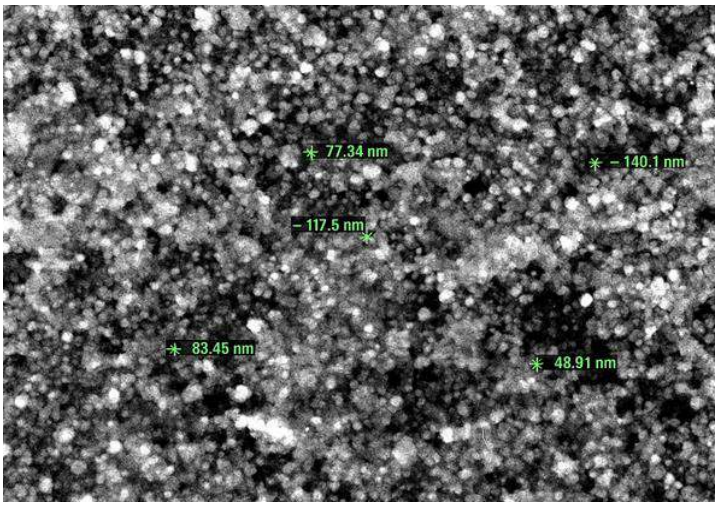

Figure 5. SEM picture of chitosan-based nanoformulations

FTIR analysis

The FTIR spectrum of the chitosan nanoformulations displayed a series of distinct absorption bands consistent with the functional groups present in chitosan. A broad band in the region associated with O–H and N–H stretching confirmed the presence of hydroxyl and amino groups, reflecting the characteristic backbone of the polymer. Prominent C–H stretching vibrations from aliphatic chains were also evident, indicating preservation of the polysaccharide structure during nanoparticle formation. The amide-related peaks, including those corresponding to amide I and amide II, suggested partial acetylation and the presence of residual amine groups. Strong C–O and C–O–C stretching bands further confirmed the integrity of the glycosidic linkages within the chitosan matrix. The slight shifts observed in certain peak positions implied possible electrostatic interactions or hydrogen bonding between chitosan and the crosslinker during nanoparticle synthesis. These spectral features collectively demonstrated that the chemical framework of chitosan remained intact while participating in the formation of stable nanoparticles (Fig. 6).

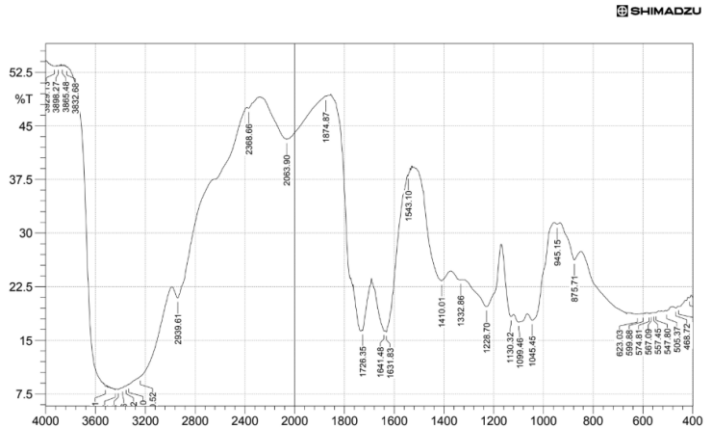

Figure 6. FTIR spectrum of chitosan-based nanoformulation

Characterization of Thymol-loaded lipid-based nanoformulations

Zeta potential and particle size

The thymol-loaded lipid nanoparticles exhibited a mean zeta potential of –16.9 mV, with the main peak occurring at –13.6 mV, indicating that the formulation carries a moderate negative charge. Although the charge is lower in magnitude compared to highly stable colloidal systems, it is sufficient to impart reasonable electrostatic repulsion and prevent rapid aggregation. The consistent scattering intensity recorded during the measurements reflects a well-dispersed population of nanoparticles and suggests minimal interference from oversized particles or aggregates. Conductivity values further supported the presence of a stable lipid matrix surrounding the encapsulated thymol molecules. Particle size analysis across intensity-, volume-, and number-based distributions confirmed that the nanoparticles remained well within the nanometer scale, with all D-values showing a narrow and controlled range. The calculated span values indicated a uniform particle population with limited variability in size. This uniformity is essential for predictable behavior in delivery applications, as consistent particle dimensions influence release characteristics and stability. Collectively, the DLS results verify that the solvent evaporation method effectively produced thymol-loaded lipid nanoparticles with desirable colloidal stability and evenly distributed nanoscale dimensions (Fig. 7).

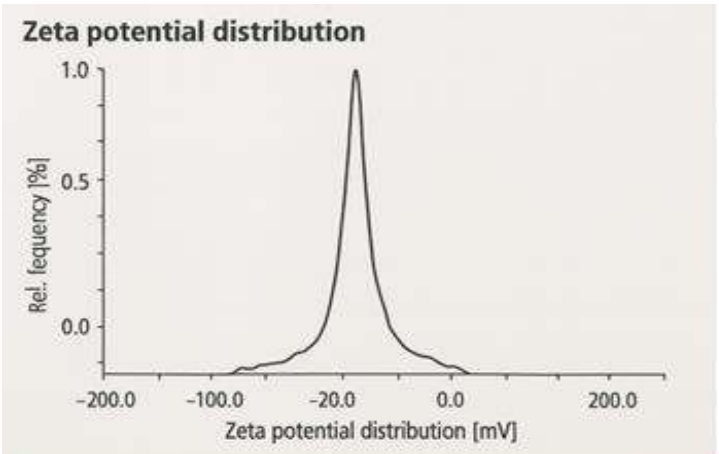

Mean zeta potential	–16.9 mV
Distribution peak value	–13.6 mV
Processed runs	3
Adjusted voltage	60.0 V
Mean intensity	277.1 kcounts/s
Electrophoretic mobility	–1.3264 µm-cm/V-s
Filter optical density	1.9081
Conductivity	1,538 m5/cm
Transmittance	2.8 %

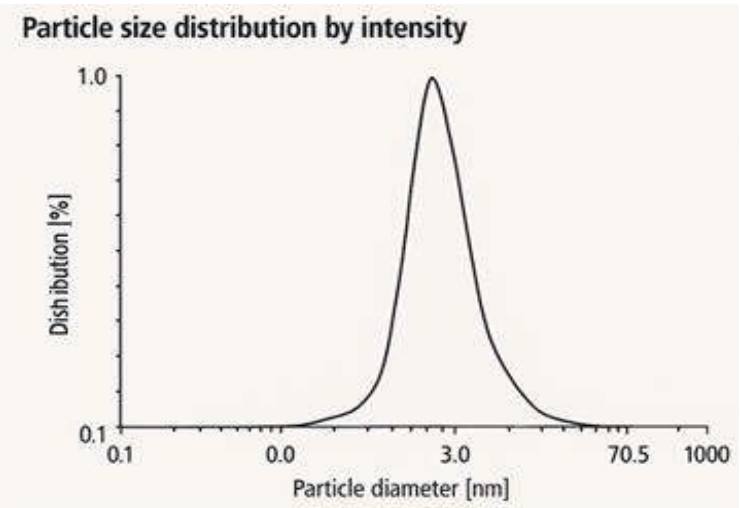

Undersize values	D_{10} [nm]	D_{30} [nm]	D_{50} [nm]	Undersize span $(D_{90}-D_0)/D_{30}$
Volume	18.02	23.45	70.35	1.594
Intensity	22.89	26.63	56.84	1.594
Number	21.20	26.41	35.12	1.594

Instrument information		
Serial number	82510602	660 nm

Figure 7. Zeta potential & particle size distribution of lipid-based nanoformulations (Thymol)

SEM analysis

The SEM images of the thymol-loaded lipid nanoformulations revealed a well-distributed population of nanoparticles with predominantly spherical shapes and occasional slight irregularities. The particles were uniformly dispersed across the examined field, with no evidence of strong agglomeration or clustering, indicating good physical stability of the formulation. Measured particle sizes ranged from approximately 84 nm to 180 nm, aligning well with the expected nanoscale dimensions for lipid-based delivery systems. The smooth surface morphology of the nanoparticles suggests that the emulsification and solvent evaporation steps were efficiently executed, allowing the lipid molecules to reorganize into compact, uniform structures. The absence of cracks, pores, or surface disruptions further confirms the structural integrity of the nanosystems. The consistent appearance of particles throughout the micrograph highlights the reproducibility of the preparation method (Fig. 8).

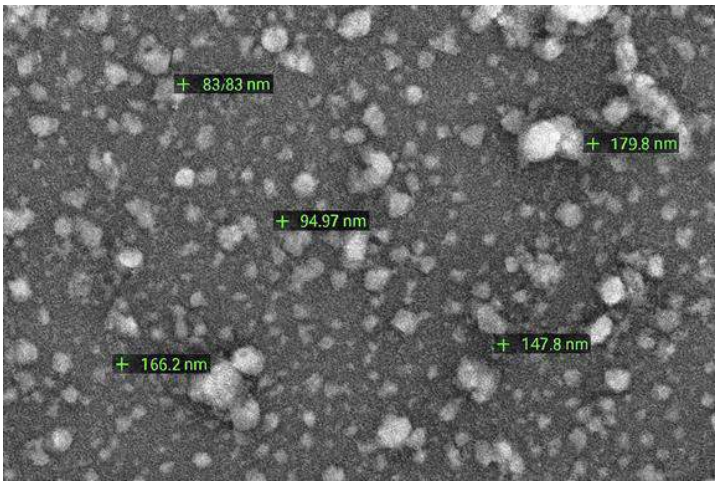

Figure 8. SEM pictureof Thymol loaded lipid-based nanoformulations

FTIR analysis

The FTIR spectrum of the thymol-loaded lipid nanoformulation showed a clear set of absorption peaks that reflected the functional groups associated with both the lipid matrix and the encapsulated thymol. A broad O–H stretching band confirmed the presence of hydroxyl groups, consistent with the phenolic structure of thymol. Distinct C–H stretching peaks indicated the saturated hydrocarbon chains of the lipid components, demonstrating that the lipid backbone remained intact after processing. A well-defined C=O stretching band suggested the presence of ester linkages, confirming the structural integrity of the lipid carriers. The appearance of aromatic C=C stretching vibrations further supported the presence of thymol within the formulation. Additional C–O and C–O–C stretching peaks were observed, characteristic of ester and ether bonds commonly found in fatty acids and surfactants used in the system. Subtle shifts in some bands implied mild interactions between thymol and the lipid matrix, possibly through hydrogen bonding or van der Waals forces. These interactions are desirable, as they indicate successful embedding of thymol within the nanostructure. The absence of disruptive new peaks suggests that no chemical degradation occurred during formulation (Fig. 9).

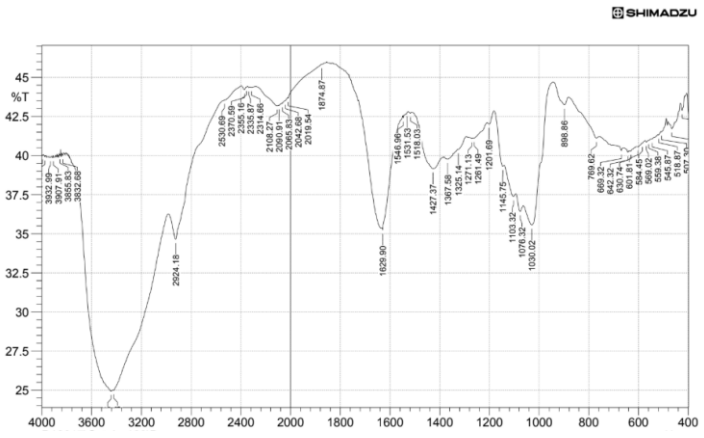

Figure 9. FTIR spectrum of Thymol-loaded lipid-based nanoformulations

Characterization of protein-based nanoformulations (Zein)

Zeta potential and particle size

The zein-based protein nanoformulations demonstrated a distinctly high positive surface charge, with a mean zeta potential of +31.5 mV and a peak centered at +33.4 mV. These values indicate strong electrostatic repulsion between particles, which is essential for maintaining a stable colloidal suspension without rapid aggregation.

The particle size data obtained from volume-, intensity-, and number-based distributions confirmed that the nanoparticles were consistently within the nanometer range. The D_{10} and D_{50} values across all analytical modes showed that a large proportion of the particles fell within smaller size classes, suggesting efficient nucleation and controlled growth during antisolvent precipitation. Although a moderate degree of polydispersity was observed, the distribution remained narrow enough to support uniform particle behavior. The combination of high zeta potential and well-defined nanoscale sizes indicates that the formulation procedure successfully yielded stable and finely dispersed zein nanoparticles. (Fig. 10).

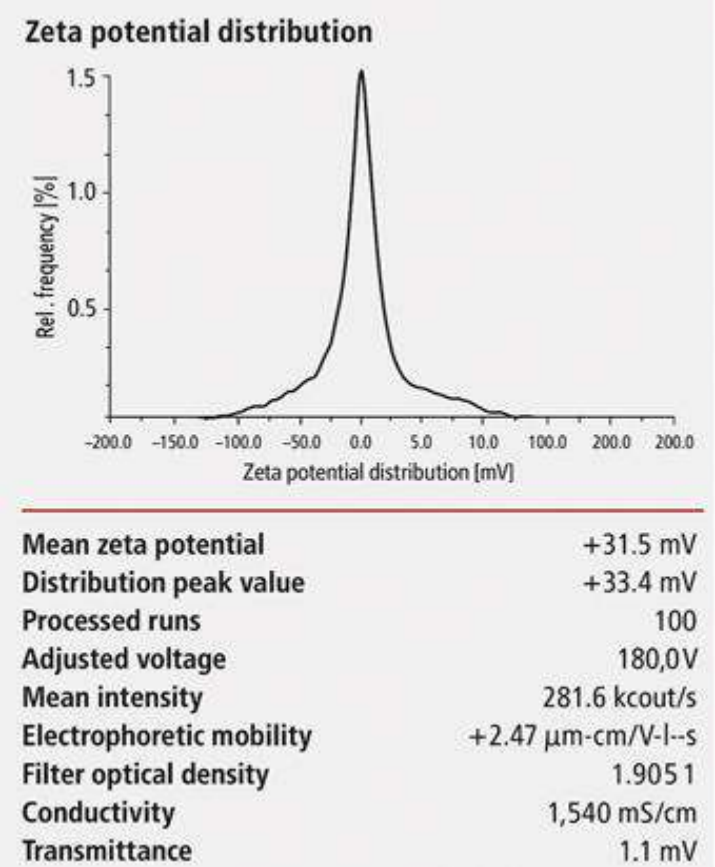

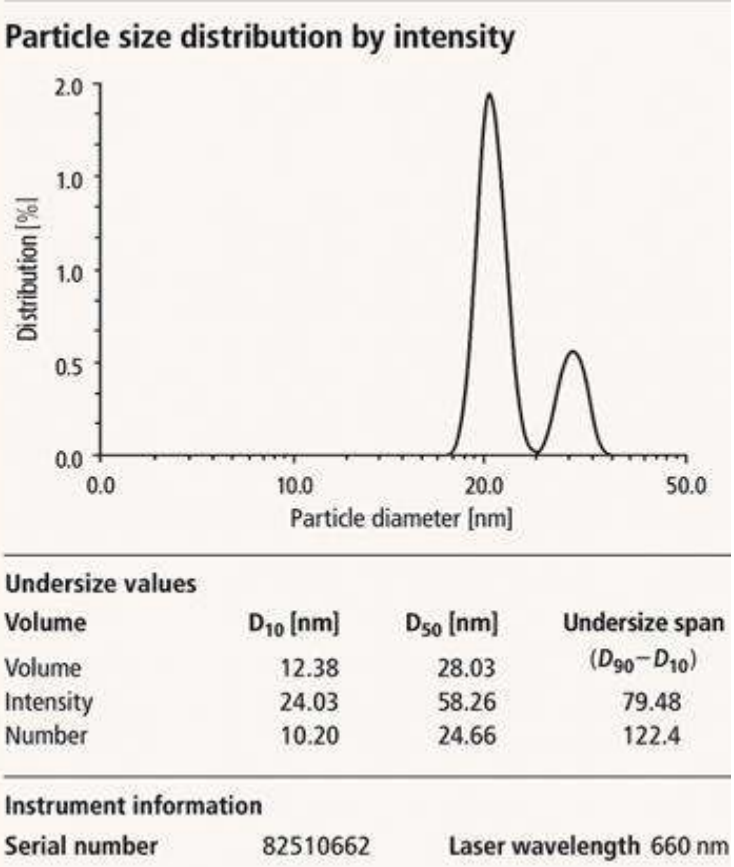

Figure 10. Zeta potential and particle size distribution of protein-based nanoformulations (Zein)

SEM analysis

The SEM examination of the zein nanoformulations revealed a uniform population of well-defined nanoparticles, predominantly spherical in shape. The measured particle sizes ranged from 66 to 94 nm, confirming their placement firmly within the nanometer scale. The particles appeared evenly distributed across the micrograph, with no noticeable clumping or aggregation, indicating effective stabilization during the antisolvent precipitation process. The smooth and compact surfaces of the nanoparticles reflected the natural self-assembling behavior of zein proteins when exposed to aqueous antisolvent conditions. This structural uniformity suggests that the formulation parameters—such as ethanol concentration, injection speed, and stirring rate—were well optimized to promote controlled nucleation and particle formation. The absence of surface defects or irregularities further highlights the integrity of the nanostructures. Such morphological regularity is advantageous in applications requiring predictable interaction with biological systems, controlled release of encapsulated compounds, or stable incorporation into food matrices (Fig. 11).

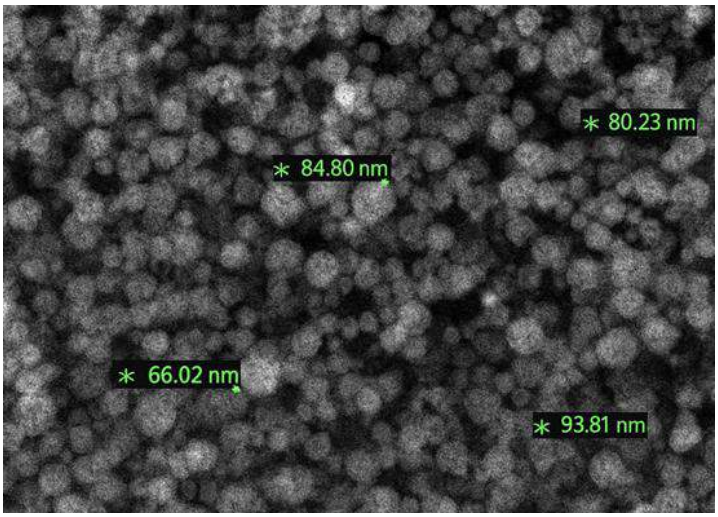

Figure 11. SEM picture of protein-based nanoformulations (Zein)

FTIR analysis

The FTIR spectrum of the zein-based nanoformulations displayed several distinct absorption bands that clearly reflected the characteristic functional groups of the protein matrix. The strong amide I band, attributed primarily to C=O stretching of peptide linkages, indicated that the core protein structure remained intact after nanoparticle formation. Similarly, the amide II band, arising from N–H bending and C–N stretching, further confirmed the preservation of zein's secondary structural elements. Peaks corresponding to C–H stretching were evident, reflecting the presence of hydrophobic aliphatic chains that are abundant within the zein protein. A broad O–H stretching region suggested hydrogen bonding interactions, possibly formed during the transition of zein from the ethanolic phase into the aqueous antisolvent. Additional mid-region C–N and C–O vibrations were observed, supporting the presence of stable protein conformations within the nanoparticles. The absence of significant peak shifts or disappearance of major protein bands indicated that the nanoparticle fabrication process did not disrupt the fundamental structure of zein. Instead, the spectral profile suggested that zein maintained its functional backbone while adapting to the nanoscale arrangement (Fig. 12).

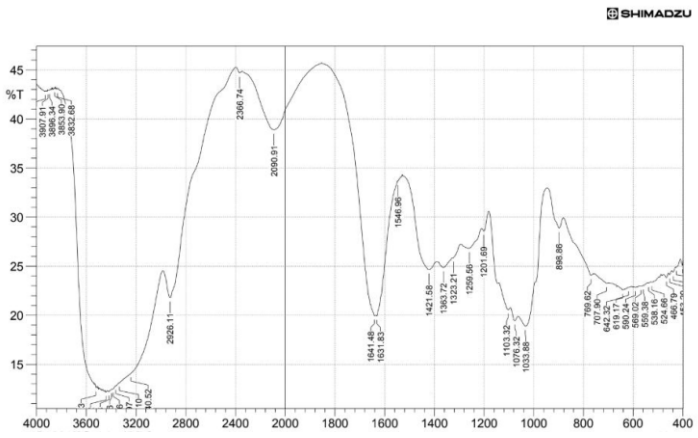

Figure 12. FTIR spectrum of protein-based nanoformulations (Zein)

Discussion

The development of edible nanoformulations using chitosan, lipids, and zein demonstrated that each biopolymer possesses unique structural and functional mechanisms contributing to successful nanoparticle formation. The ionic gelation process used for chitosan resulted in nanoparticles with a markedly high positive surface charge, indicating strong stability and well-maintained dispersion. Chitosan is well known for its cationic nature in mildly acidic environments due to protonation of free amino groups, which promotes electrostatic stability and prevents aggregation—a behavior widely reported in earlier studies [16, 17). The narrow particle size distribution obtained for these nanoparticles reflects efficient crosslinking between chitosan and TPP, a phenomenon attributed to rapid ionic interaction and the formation of a tightly bound network, consistent with observations from recent nanodelivery research [18]. The morphological characteristics confirmed through SEM analysis further emphasized the efficiency of ionic gelation, as chitosan nanoparticles exhibited smooth surfaces and well-defined spherical shapes. Such observations align with previous work demonstrating that ionic gelation often yields uniform nanoscale structures with limited surface defects, making them suitable for bioactive delivery and antimicrobial coating applications [19]. FTIR findings also supported nanoparticle formation by showing slight shifts in functional groups indicative of intermolecular interactions between chitosan and the crosslinker. These interactions, often in the form of hydrogen bonding or electrostatic attraction, are essential for structural stability and have been documented in the literature describing chitosan-based encapsulation systems [20].

Thymol loaded Lipid-based nanoformulations also demonstrated successful nanoparticle synthesis, as confirmed by both DLS and SEM analyses. The moderate negative zeta potential (–16.9 mV) of these nanoparticles suggests that the formulation relies on a combination of electrostatic and steric stabilization provided by surfactants like Tween 80. Similar stabilization patterns have been reported in solid lipid nanoparticles and nanostructured lipid carriers developed for encapsulating hydrophobic compounds [21, 22]. The nanoscale dimensions observed across particle size measurements reflect efficient emulsification and solvent evaporation processes, enabling stable lipid reorganization during formulation. Previous reports also highlight that the solvent evaporation technique yields nanoparticles with well-controlled size distribution, particularly when bioactive compounds such as essential oils are incorporated [23].

SEM imaging of lipid nanoparticles reinforced the DLS results, showing consistently shaped spherical particles with minimal aggregation. The smooth surfaces observed suggest proper lipid solidification and stabilization, a feature crucial for achieving controlled release and enhancing the bioavailability of hydrophobic compounds. Studies examining thymol- and carvacrol-loaded lipid nanoparticles have similarly demonstrated that lipid matrices can encapsulate phenolic compounds without compromising their structural attributes [24]. FTIR spectra further validated this, confirming the presence of functional groups corresponding to both lipids and thymol and demonstrating that encapsulation preserves the chemical integrity of the bioactive. Comparable findings in current literature show that lipid nanocarriers retain essential functional groups of the encapsulated molecules while forming stable ester- and ether-based interactions within the matrix [25].

Zein-based nanoparticles demonstrated strong positive zeta potentials and excellent structural integrity, reflective of the protein's amphiphilic nature. Zein is known to self-assemble into spherical nanoparticles due to its high hydrophobic amino acid content—a phenomenon driven by hydrophobic interactions and hydrogen bonding when dissolved in ethanol and introduced into water [26]. The nanoscale dimensions of the zein nanoparticles in this study align with findings that antisolvent precipitation produces tightly packed protein nanostructures suitable for carrying hydrophobic and moderately hydrophilic compounds [27]. SEM analysis further confirmed the ability of zein to form monodisperse, smooth nanoparticles without aggregation, an observation frequently reported in studies involving zein nanocarriers for food-grade bioactives and antioxidants [28]. FTIR spectra of zein nanoparticles indicated well-preserved amide I and II regions, confirming that secondary structures remained intact during nanoparticle formation. This retention of structure is significant for maintaining the functional capabilities of zein as a delivery vehicle, as it preserves the protein's ability to bind or encapsulate bioactive compounds efficiently. Previous analyses also show that antisolvent precipitation maintains the α-helical structure of zein, ensuring stability of the resulting nanosystem [29]. When comparing the three nanoformulation systems, it becomes evident that chitosan produced the strongest electrostatic stability due to its higher surface charge, while zein nanoparticles exhibited stability due to protein self-assembly behaviours. Lipid nanoparticles, though possessing lower zeta potentials, benefited from steric stabilization and dense core formation, resulting in adequate colloidal stability. Across all systems, FTIR and SEM analyses confirmed structural integrity, successful encapsulation, and effective nanoparticle formation.

Conclusion

The present investigation demonstrated that three distinct green synthesis approaches—ionic gelation, solvent evaporation, and antisolvent precipitation—can effectively produce edible nanoformulations with favorable physicochemical and structural attributes. Chitosan nanoparticles prepared by ionic gelation exhibited high colloidal stability, as reflected by their strong positive surface charge and uniform nanoscale size distribution. Lipid-based nanoparticles containing thymol formed a stable, well-dispersed system with consistent particle morphology and clear spectral evidence of intact lipid and bioactive functional groups. Zein nanoparticles generated through antisolvent precipitation displayed controlled self-assembly, high surface charge, and preserved protein structural features, confirming the suitability of the method for protein-based nanocarrier development. SEM imaging across all formulations verified well-defined nanoscale morphology with minimal aggregation, while FTIR spectra confirmed that the core chemical structures of chitosan, lipids, and zein were retained following nanoparticle formation. Collectively, these findings highlight the effectiveness of the selected fabrication techniques in producing stable, monodisperse, and structurally sound edible nanoparticles. The resulting systems offer significant promise for applications in functional foods, nutraceutical delivery, natural preservatives, and controlled-release formulations, providing a strong foundation for future development of safe and efficient bioactive carriers.

Acknowledgement: The Authors would like to thank the HoD of Microbiology and Management of Bhavan's Vivekananda College of Science, Humanities and Commerce for the support and encouragement to carry out the research work in the college.

Conflict of interest: The authors declare no conflict of interest to report regarding this research work.

References

1. Lei, Y., Huang, H., Xiao, M., Chen, X., & Yu, H. (2024). Nanoencapsulation and delivery of bioactive ingredients in food applications: Recent advances and future trends. Comprehensive Reviews in Food Science and Food Safety, 23(1), 1–34.
2. Vanaraj, R., Arumugam, S., Subramanian, S., Nagarajan, S., &Thangam, R. (2024). A current trend in efficient biopolymer coatings for edible packaging: Opportunities and challenges. Foods, 13(7), 1158
3. Gupta, D., Verma, S., Singh, R., & Mathur, A. (2024). Plant-based edible films and coatings for food-packaging applications: Recent advances and future challenges. Food & Function, 15(4), 1890–1915.
4. Jafarzadeh, S., Iravani, S., Varma, R. S., Shekarforoush, E., &Rohani, S. M. (2024). Green synthesis of nanomaterials for smart biopolymer films in food packaging applications. Journal of Nanostructure in Chemistry, 14, 1–28.
5. Karnwal, A., Kaur, M., Sharma, A., & Chopra, K. (2025). Natural biopolymers in edible coatings: Applications, functionality, and future perspectives. Current Research in Food Science, 9, 100247.
6. Hojabrean, M., Hosseinifarahi, M., Radi, M., & Amiri, S. (2025). Enhancing storage quality of fresh-cut cucumbers using thymol-loaded Ca-alginate films: Nanoemulsion versus nanostructured lipid carriers. Applied Food Research, 12, 101208.
7. Hoang, N. H., Nguyen, T. T. H., Pham, M. H., Tran, T. T., Le, T. T., & Pham, T. D. (2022). Chitosan nanoparticles-based ionic gelation method and their agricultural applications: A review. Nanomaterials, 12(5), 852.
8. Lorevice, M. V., Otoni, C. G., & Moura, M. R. (2016). Chitosan nanoparticles on the improvement of thermal, barrier, and mechanical properties of pectin-based films. Food Hydrocolloids, 52, 732–740.

9. Algarni, E. H. A., Al-Turk, W. A., & Alharbi, M. (2022). Effect of chitosan nanoparticles as edible coating on the quality and shelf life of apricot fruits. Polymers, 14(11), 2227.
10. Melo, N. R., Muniz, C. R., Santos, J. S., Almeida, F. D. L., & Costa, M. J. (2020). Comparative effect of fungal chitosan gel, nanoparticles and gel–nanoparticles as edible coating on fresh fruits. ISEKI Food e-Journal, 19, 1–12.
11. Blanco-Llamero, C., Fonseca, J., & Prieto, G. (2022). Nutraceuticals and food-grade lipid nanoparticles: A new alliance for health. Foods, 11(15), 2318.
12. Lüdtke, F. L., Schneider, J. F., Barbosa, L. N., Castro, I. A., & Pinto, U. M. (2025). Lipid nanoparticles: Formulation, production methods and applications in food systems. Nanomaterials, 15(1), 112.
13. Pascoli, M., De Carvalho, S. M., Pereira, S., & Costa, A. L. (2018). Zein nanoparticles and strategies to improve their colloidal stability: A review. Frontiers in Chemistry, 6, 6.
14. Oleandro, E., Baldino, L., Scognamiglio, M., Reverchon, E., &Mangiacapra, P. (2024). Zein-based nanoparticles as active platforms for food and biomedical applications: A comprehensive review. Nanomaterials, 14(5), 414.
15. Spasojević, L., Pajić, M., Vukosavljević, P., Tomić, N., &Lazić, V. (2019). Edible water barrier films prepared from aqueous dispersions of zein nanoparticles. Journal of Food Science, 84(9), 2582–2592.
16. Abdelhamid, H. N., & Wu, H. F. (2020). Chitosan-based nanomaterials for drug delivery and biomedical applications. International Journal of Biological Macromolecules, 154, 214–233.
17. Dash, M., Chiellini, F., Ottenbrite, R. M., & Chiellini, E. (2019). Chitosan—A versatile semi-synthetic polymer for nanomedicine. Progress in Polymer Science, 102, 101–125.
18. Bakshi, P. S., Selvakumar, D., &Kadirvelu, K. (2021). A review on chitosan-based nanoparticles for drug delivery applications. Carbohydrate Polymers, 264, 118–147.
19. Khan, M. I., Gani, A., Masoodi, F. A., Amin, F., Wani, S. M., & Naik, H. R. (2020). Chitosan nanoparticles as potential nanocarriers for natural preservatives: Preparation and characterization. Journal of Food Science and Technology, 57, 233–244.
20. Ribeiro, A. M., Estevinho, B. N., Rocha, F., & Santos, D. (2020). Solid lipid nanoparticles as a delivery system for lipophilic bioactives: Advances and perspectives. Journal of Functional Foods, 67, 103–116.
21. Salvi, V. R., Kulkarni, V. K., Yadav, D., & Anand, R. (2022). Lipid nanoparticles for improved bioavailability of hydrophobic compounds. Advanced Drug Delivery Reviews, 184, 114–125.
22. Eghbaliferiz, S., Shojaee-Aliabadi, S., Hosseini, S. M., Ghasemi, I., & Alizadeh, A. (2021). Essential oil-loaded lipid nanocarriers: Stability, release, and food applications. Colloids and Surfaces B: Biointerfaces, 203, 111771.
23. Sharma, N., Chaudhary, P., Kumar, S., Rana, S., & Sehgal, A. (2021). Lipid-based delivery systems for essential oils: Applications in food preservation. Food Chemistry, 343, 128556.
24. Yuan, Y., Li, J., Xu, Y., Xu, H., &Xiong, Y. (2020). Nanostructured lipid carriers for effective encapsulation of phenolic compounds. Trends in Food Science & Technology, 99, 580–595.
25. Patel, A. R., Heussen, P., Dorst, E., Hazekamp, J., &Velikov, K. P. (2020). Protein-based nanoformulations for delivery of nutraceuticals: A review. Food Hydrocolloids, 105, 105–126.
26. Li, M., Piao, X., Li, X., Ma, L., Kim, Y. J., & Chen, X. (2021). Zein nanoparticles for encapsulation of food ingredients: Preparation, properties, and applications. Critical Reviews in Food Science and Nutrition, 61, 139–157.
27. Bourbon, A. I., Pinheiro, A. C., & Vicente, A. A. (2020). Zein nanoparticles as edible carriers for bioactive compounds. Food Research International, 137, 109728
28. Azevedo, M. A., Bourbon, A. I., & Vicente, A. A. (2022). Zein-based nanoformulations for the delivery of food bioactives: Structural and functional insights. Food Hydrocolloids, 124, 107296.
29. Wu, C., Li, Y., Zhao, X., Chen, H., & Wang, Y. (2016). Edible coating from citrus essential oil–loaded chitosan nanoparticles for preservation of silvery pomfret. RSC Advances, 6(36), 32586–32596.